

Photoacoustic Active Ultrasound Element for Catheter Tracking

Xiaoyu Guo, Behnoosh Tavakoli, Hyun-Jae Kang, Jin U. Kang, Ralph Etienne-Cummings and Emad M. Bector

^aDept. of Electrical and Computer Engineering, Johns Hopkins University, Baltimore, MD, USA

^bDept. of Computer Science, Johns Hopkins University, Baltimore, MD, USA

^cDept. of Radiation Oncology, Johns Hopkins University, Baltimore, MD, USA

ABSTRACT

In recent years, various methods have been developed to improve ultrasound based interventional tool tracking. However, none of them has yet provided a solution that effectively solves the tool visualization and mid-plane localization accuracy problem and fully meets the clinical requirements. Our previous work has demonstrated a new active ultrasound pattern injection system (AUSPIS), which integrates active ultrasound transducers with the interventional tool, actively monitors the beacon signals and transmits ultrasound pulses back to the US probe with the correct timing. *Ex vivo* and *in vivo* experiments have proved that AUSPIS greatly improved tool visualization, and provided tool-tip localization accuracy of less than 300 μm . In the previous work, the active elements were made of piezoelectric materials. However, in some applications the high driving voltage of the piezoelectric element raises safety concerns. In addition, the metallic electrical wires connecting the piezoelectric element may also cause artifacts in CT and MR imaging. This work explicitly focuses on an all-optical active ultrasound element approach to overcome these problems. In this approach, the active ultrasound element is composed of two optical fibers - one for transmission and one for reception. The transmission fiber delivers a laser beam from a pulsed laser diode and excites a photoacoustic target to generate ultrasound pulses. The reception fiber is a Fabry-Pérot hydrophone. We have made a prototype catheter and performed phantom experiments. Catheter tip localization, mid-plan detection and arbitrary pattern injection functions have been demonstrated using the all-optical AUSPIS.

Keywords: Ultrasound, Catheter Tracking, Photoacoustic, Image guided surgery

1. INTRODUCTION

Localizing the needle tip is a crucial task that affects safety and effectiveness of medical interventional procedures, such as biopsy, cardiac catheterization, IVF, etc [1]. MRI, CT and ultrasonography are most widely used in clinic among all image guidance modalities [2]. Compared with other modalities, ultrasonography has its merits of cost, safety, mobility and usability. However, it has two major limitations when used in tool guidance applications. The first one is poor visualization. Ultrasonography reconstructs images from received echo ultrasound signals. In interventional procedures, the reflected acoustic waves from many catheters or needles are very weak, or highly angle dependent due to their size and geometry. As a result, these surgery tools cannot be reliably visualized in ultrasound images. The second limitation is the low localization accuracy. Most medical ultrasound systems work at a frequency of 1~10MHz. The acoustic beam width usually ranges from several millimeters to one centimeter, which means an object shown on a 2D ultrasound image has an inherent uncertainty of a few millimeters to one centimeter along the elevation axis [3]. Therefore, for interventional procedures requiring sub-millimeter tracking accuracy conventional ultrasonography cannot be used.

In recent years, several approaches have been developed to improve tool visualization and pose recovery with ultrasonography, including optical tracking, electromagnetic (EM) tracking, beam steering, passive and active ultrasound markers [4-11]. The optical tracking approach suffers from several limitations including high cost, calibration complexity, intrusive setup, and the need for clear line-of-sight from the camera to the tool [5]. EM tracking approach has been recently introduced and integrated into several commercial ultrasound scanners (GE LOGIQ E9, Ultrasonix GPS, etc.). It has an excellent off-plane detection capability [6]. However, it has several limitations such as: the overall navigation accuracy can easily be worse than 2~3mm; it requires specially designed imaging equipment; and any ferromagnetic object in the operation region may affect system accuracy. Another approach with a similar concept is to use ultrasound sensors instead of EM sensors. The drawback is that it is not a standalone device and requires a major modification of the ultrasound imaging system. Instead of detecting the tool spatial location using a separate system,

some researchers focus on the visualization enhancement of the catheter in B-mode images. One approach is the beam steering method that is effective when the catheter is in-plane. But for cases where catheters simply intersect the imaging plane, this method is not effective. Another approach is to improve image quality by using passive ultrasound markers. The major issue of this approach is that visualization enhancement by scattering coating is limited, and markers are usually too bulky for small catheters [7]. On the other hand, active ultrasound marker approach has also been proposed. F. Simonetti introduced the concept of using biopsy needles as ultrasound waveguide [11]. The limitation of this method is that the phase, waveform, timing and leaking position of the guided beam cannot be well controlled; it requires that the ultrasound system stop the normal operation and work in passive mode, which is not a direct visualization enhancement; its performance highly relies on the mechanical property of the needle, and cannot be generally applied to any surgery tools. B. Breyer and I. Cikes reported an active ultrasound marker system that fires an ultrasound signal from the catheter, which shows a visible spot in the B-mode image [12]. This work for the first time proposed the active reflection concept in ultrasound imaging. However, this method was not actually used in clinics. Experiment results show that in the *in vivo* B-mode images, it is difficult to identify the active echo spot from the tissue texture. Even in the water tank environment, a simple receive and echo configuration does not provide enough feedback to the operator since the echo spot may show up within a large range of tool positions, which decreases localization accuracy.

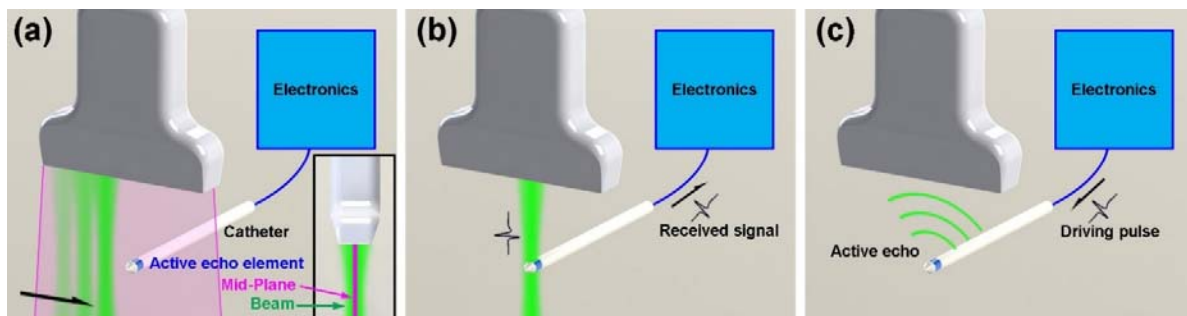


Fig. 1. The mechanism of active echo. a) The imaging probe fires a series of ultrasound beams scanning the image region. The center plane of the image region is the mid-plane. b) When an ultrasound beam scans over the active echo element, an electrical signal is received by the electronics. c) The signal triggers the electronics, a driving pulse drives the element to fire an active echo pulse.

In our previous work, we presented a new technique called active ultrasound pattern injection [13]. In contrast to other approaches, the tool visualization and localization is not simply achieved by inducing an ultrasound beam to the tissue or echoing the imaging pulses. The Active Ultrasound Pattern Injection System (AUSPIS) is composed of an interventional tool integrated with active echo (AE) elements, ultrasound analog frontends, a signal processing system, and a multichannel pulser. The active echo element is a miniaturized omnidirectional ultrasound transducer. As shown in figure 1, when the US system is acquiring a B-mode image, probe elements fire sequentially to scan the entire field of view (FOV). If an active echo element is in the FOV, it will sense the beacon pulse when the transmission beam scans over.

The AUSPIS solves both of the two major problems in US interventional tool tracking at the same time. Firstly, to improve tool visualization, the AUSPIS will drive the AE element to send a US pulse immediately after the beacon signal is received. Since the reception-transmission delay is in nanoseconds and negligible for US imaging, the US pulse is superimposed on the catheter echo wave, results in an enhanced echo pulse with a much higher amplitude, broader frequency range and wider emission angle, travels back to the imaging probe, and appears as a bright spot (AE spot) that indicates the AE element location in the B-mode image. We have also developed the time and frequency modulation method to further improve visualization enhancement. Secondly, to improve tool tracking accuracy, especially along the elevation axis, AUSPIS has a Mid-Plane Detection function, which results in a localization accuracy beyond the ultrasonography imaging resolution, as shown in figure 2. Since the AE element is capable of measuring the local ultrasound pressure in real time, the beam intensity distribution can be utilized to localize the mid-plane. When the active echo element is well aligned with the central plane, the received beacon signal amplitude reaches its maximum, and when it moves away the strength of beacon is decreased. In our previous *ex vivo* and *in vivo* experiments, using AUSPIS with piezoelectric AE element, the catheter tip localization accuracy is constantly less than 300 μm .

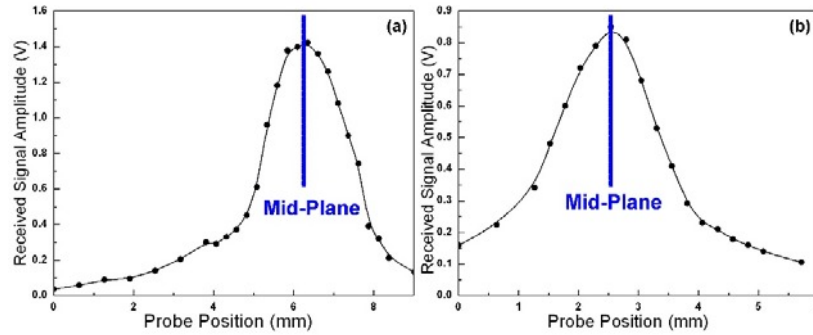


Fig. 2. The local ultrasound amplitude measurement for mid-plane detection. The amplitude of the signal received by the active echo element versus the position of the probe. The depth of the US transmission beam focus is close to the catheter to probe distance, the two plots are showing the signal distribution near the focus. a) The results with catheter perpendicular to the image plane (off-plane) b) catheter parallel to the image plane (in-plane).

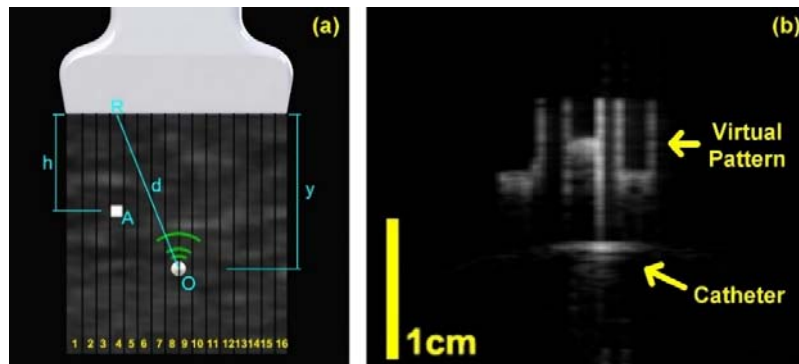


Fig. 3. B-mode Pattern injection with a linear array. a) A illustration of how a virtual pixel is injected into the B-mode image from an AE element. Since the AE element has a wide emission angle, the AE signal can be received by the entire probe array. By applying a proper reception-transmission delay, the AE element *O* fires a US pulse when the US system is acquiring the line#4, and a virtual spot is shown at position *A* in line#4. b) An example B-mode image with a virtual pattern. The spot near the image bottom is the echo signal from the catheter, which is perpendicular to the image plane. The "JHU" character is a virtual pattern injected from a single active US element integrated on the catheter. The experiment is performed in a water tank, image is acquired by a Sonix CEP system running in general B-mode with a L12-5 linear probe.

Moreover, AUSPIS can also interact with the US imaging system in more intelligent ways. In the arbitrary pattern injection mode, as shown in figure 3, the system receives the beacon signal and fires a series of active echo pulses from the same active echo element with a proper timing, frequency, duration and amplitude. Thus it enables us to inject any "virtual" pattern into the B-mode image.

In our previous AUSPIS prototype, the AE element is made of piezoelectric materials. They are low cost, easy to fabricate and very sensitive to ultrasound signals. However there are also drawbacks. First, some interventional catheters have very small diameters, some are less than a few hundred microns. It is difficult to make a piezoelectric AE element with its electrical wire connections and isolations within that size. Second, driving a piezoelectric element requires electrical pulses with a duration of tens to hundreds nanoseconds and a voltage of 20-50 volts. This may raise safety concerns in some applications. Third, the piezoelectric element and the metal wires may cause artifacts when using with CT and MRI systems.

To overcome these problems, a more compact, non-electrical solution is needed. In this paper, we introduce an all-optical AUSPIS design. The piezoelectric AE element is replaced by two separate US sensors and transmitters, both of which are fiber optical based devices. The sensor receives the ultrasound pulse and converts it to an optical signal, which is picked up by an external optical system and turned into an electrical signal to trigger the AUSPIS controller circuit. On the transmission side, AUSPIS controls a laser source to send optical pulses. Ultrasound wave is generated through the

photoacoustic (PA) effect. This paper details the all optical AUSPIS design, the exploration of fiber based PA transmitter, and the lab bench system experiment results.

2. METHODS

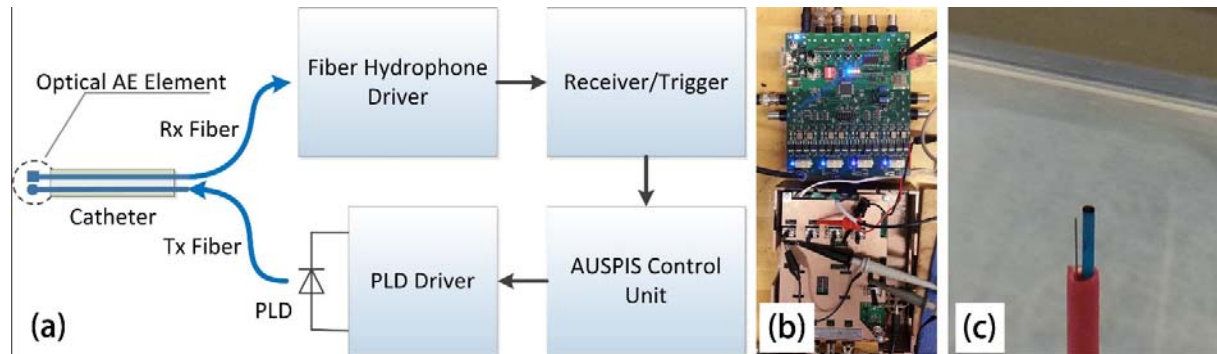


Fig. 4. Optical AUSPIS prototype setup. a) System diagram. b) AUSPIS controller (top) and the receiver/trigger (bottom) c) Tx (the thicker one) and Rx fiber tips on the catheter end.

Figure 4 shows the configuration of the optical AUSPIS prototype. The system is composed of a catheter with a Tx and Rx fiber integrated, a fiber hydrophone driver, a signal receiver/trigger, an AUSPIS control unit, a pulsed laser diode (PLD) driver, and a PLD with a fiber coupling system. The Rx fiber with the fiber hydrophone driver is a commercialized product developed by Precision Acoustics. LTD. On the fiber tip, multiple reflection layers are coated to form a Fabry-Pérot interferometer [14]. When an ultrasound beam is introduced, the layers vibrate with the ultrasound wave and cause variation of the interference laser beam intensity. The fiber hydrophone driver receives the optical signal and converts it to an analog electrical signal. This optical hydrophone system has a detection bandwidth from 250 kHz to 50 MHz, a dynamic range from 10kPa to 15MPa, and sensitivity about 150mV/MPa. The output from the fiber hydrophone system is sent to a receiver/trigger that we developed. This device amplifies and filters the signal to increase the SNR and amplitude for further signal processing. A trigger circuitry is also implemented to generate a TTL pulse when the signal amplitude exceeds an adjustable threshold. Because the main peak of the ultrasound can be either positive or negative, the trigger circuitry is designed to be able to pick up the peaks with absolute amplitude above a certain threshold. The output from the receiver/trigger goes to the AUSPIS control unit, in which an embedded processor monitors the signal in real time and controls the light source to fire laser pulses with a desired timing. To inject a virtual pattern, the AE element needs to send ultrasound pulses based on the received beacon signal. Since the AUSPIS is a stand alone system, the beacon signal from the US imaging system is totally unpredictable. This requires the AE element being ready to fire at any time, capable to run at a high repetition rate and adjustable pulse width. Conventional Q-switch lasers widely used in PA systems do not meet the requirements. Diode lasers have merits of high repetition rate, flexible pulse duration and no pumping delay. The major drawback is the pulse energy, which is typically four to five orders lower than that of Nd:YAG Q-switch lasers. With such a low energy, the generated PA pulses may barely be visualized in the B-mode image. In this system, we use a multi-junction high power pulsed laser diode (PLD) 905D3S3j09, which is optimized for high peak power pulsed mode operation. A customized laser diode driver with a maximum output voltage of 150V and current of 300A is designed and built. The pulsed laser diode emission has a wavelength of 905 ± 10 nm, a peak output power of 200W, and a divergence angle of 20 degree. An aspherical lens pair is used to couple the laser beam to the Tx fiber, which has a core size of 200 μ m. The fiber output is painted with Indian ink, so the dried ink layer will absorb the laser energy and generate PA pulses.

The catheter used in this experiment is a rubber tube with a diameter of 1.5mm. Both Tx and Rx fibers are integrated inside the tube, and the fiber tips are fixed at the same position. In the experiment, the laser pulse duration is configured to 50~100ns. So the maximum pulse energy delivered to the active echo element can be estimated by:

$$E_{pulse} = P_{max} \times t_{pulse} \times \alpha$$

where P_{max} is the maximum power, t_{pulse} is the pulse duration, and α is the coupling efficiency.

3. RESULTS

3.1 Laser power and coupling efficiency measurement

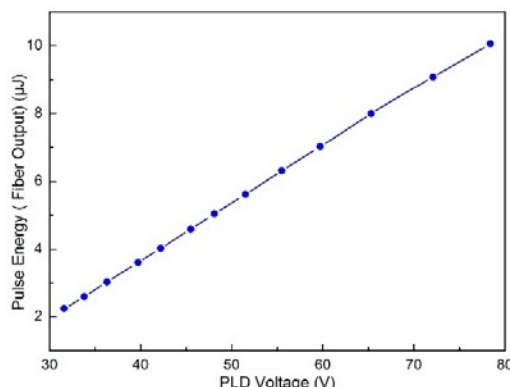


Fig. 5. The Tx fiber output laser pulse energy at different PLD driving voltages. In the energy output test the PLD is driven with a pulse duration of 100 ns and repetition rate of 500Hz.

Figure 5 shows the output energy from the Tx fiber tip (without PA coating) versus the driving voltage from 30V to 80V. Within this range, the pulse energy is roughly linear proportional to the driving voltage. The output power is very close to the specified maximum at 80V; high voltage was not tested to avoid PLD damage. We have also measured the PLD direct output energy, which is about two times higher than the fiber output. So the coupling efficiency is about 50%.

3.2 Mid-Plane Detection

In the all-optical AUSPIS, the AE element receiving aperture is about 10 μm , which is the size of the Rx fiber tip. This is smaller than our previous piezoelectric AE element. The small Rx aperture results in a higher spatial signal resolution, so the Mid-plane detection accuracy is further improved. In water tank tests, based on the feedback from the AUSPIS, the catheter tip can be localized to the B-mode image mid-plane with an accuracy of 100 μm .

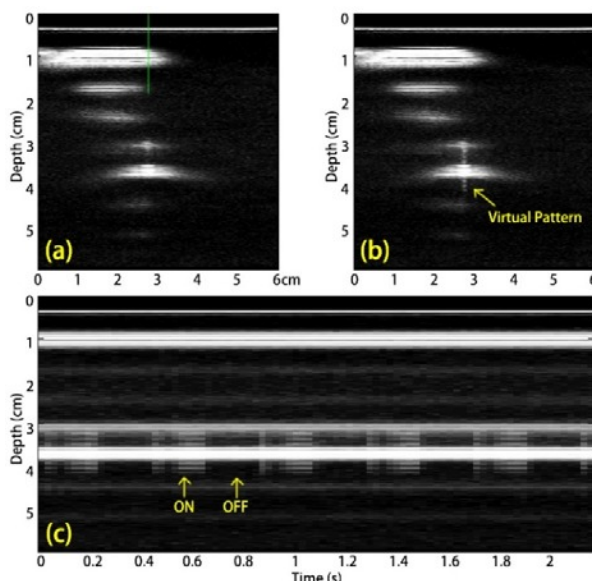


Fig. 6. Images of virtual pattern injection by the optical AUSPIS. a) The B-mode image when AUSPIS is off. b) The B-mode image with AUSPIS turned on. A virtual bar pattern is injected in the image. c) The M-mode image of the virtual pattern injection. The AUSPIS is turned on and off periodically. The M-mode line position is indicated by the green line in (a). From the M-mode image the injected pattern variation can be seen clearly.

3.2 Pattern Injection

Figure 6 shows the image of virtual pattern injection by the optical AUSPIS. The data is acquired by a Sonix CEP ultrasound imaging system with a L14-5W linear probe. The experiment is performed in a water tank. The catheter is placed vertically, the tip is indicated by the spot close to the center of the B-mode image. The bright bands in the image come from the catheter holder. In figure 6, the AUSPIS control unit is running in the central plane indication mode. The system detects the beacon signal from the imaging probe and injects virtual bars while the number of bars indicates the signal amplitude. Central plane can be found by adjusting the catheter position to maximize the bars. Comparing Figure 6 (a) and (b), the virtual bar can be seen clearly when AUSPIS is turned on. The M-mode image provides a better illustration about how the injected pattern changes over time when the AUSPIS is turned on and off periodically.

4. DISCUSSIONS

The experiment demonstrated the concept of all optical active echo catheter. Compared with our previously developed piezoelectric element based system, the all-optical setup has two drawbacks. First, the ultrasound pulses generated by the PA element is much weaker than the piezoelectric element. Second, the sensitivity of the optical fiber hydrophone is lower. The first problem can be solved in different ways, like using more powerful laser sources, highly efficient PA materials, improving the coupling efficiency, etc. PLD stacks with kilowatt level output are commercially available. Multiple PLDs with a fiber beam combiner is also a simple way to multiplex the power. The pulse energy can be improved by 1 to 2 orders by these methods. The second problem can be solved by implementing more sensitive optical hydrophone and improving the receiver signal to noise ratio. Due to the miniaturized size of the all-optical AE element, it is not difficult to integrate multiple AE elements on the interventional tool. In this case, not only the tool position, but also the pose and shape, can be tracked using the AUSPIS.

5. SUMMARY

We demonstrated an active ultrasound pattern injection system using all optical active echo element. This system further reduced the size of the active echo element, avoided the metal components on the catheter and the high driving voltage of the piezoelectric element, and improved localization accuracy due to the reduced receiving aperture. Further work will explore the integration of the high power PA transmitter, high sensitivity optical ultrasound receiver, and multiple optical AE element AUSPIS tool pose recovery.

ACKNOWLEDGEMENTS

Financial support was provided by Johns Hopkins University internal funds and NIBIB-NIH grant EB015638.

REFERENCES

- [1] JE Fishman, C Milikowski, US-guided core-needle biopsy of the breast how many specimens are necessary, *Radiology* 2003; 226:779–782
- [2] GD Dodd III, MC Soulen, et al. Minimally invasive treatment of malignant Hepatic Tumors: at the threshold of a major breakthrough, *Radio Graphics* 2000; 20: 9-27
- [3] CJ Harvey, T Albrecht, Ultrasound of focal liver lesions. *Eur. Radiol.*(2001)11: 1578-1593
- [4] S Cheung, R Rohling, Enhancement of needle visibility in ultrasound-guided percutaneous procedures, *Ultrasound in Med. & Biol.*, Vol. 30, No. 5, pp. 617–624, 2004
- [5] C Chan, F Lam, R Rohling, A needle tracking device for ultrasound guided percutaneous procedures, *Ultrasound in Med. & Biol.*, Vol. 31, No. 11, pp. 1469–1483, 2005
- [6] J Krucker, S Xu, et. al. Electromagnetic tracking for thermal ablation and biopsy guidance: clinical evaluation of spatial accuracy, *J Vasc Interv Radiol* 2007; 18:1141–1150
- [7] J Stoll, P Dupont, Passive Markers for Ultrasound Tracking of Surgical Instruments, *MICCAI* 2005, LNCS 3750, pp. 41 – 48, 2005.
- [8] D Vilkomerson, D Lyons, A system for ultrasonic beacon-guidance of catheters and other minimally-invasive medical devices, *IEEE Transactions on Ultrasonics, Ferroelectrics, and Frequency Control*, vol. 44, no. 1, Jan 1997
- [9] CL Merdes, PD Wolf, Locating a catheter transducer in a three-dimensional ultrasound imaging field, *IEEE Transactions on Biomedical Engineering*, vol. 48, no. 12, Dec 2001

- [10] J Mung, F Vignon and A Jain, A Non-disruptive Technology for Robust 3D Tool Tracking for Ultrasound-Guided Interventions, MICCAI 2011, Part I, LNCS 6891, pp. 153–160.
- [11] F. Simonetti, A guided wave technique for needle biopsy under ultrasound guidance, Proc. of SPIE Vol. 7261 726118-1, 2009
- [12] B Breyer and I Cikes, Ultrasonically marked catheter—A method for positive echographic catheter position identification, Med. Biol. Eng. Comput., vol. 22, pp. 268–271, May 1984.
- [13] X. Guo, R. Etienne-Cummings, H-J. Kang, M. A. L. Bell, E. M. Boctor, Localizing Surgical Tools with an Ultrasound-based Active Reflector Tracking System, UITC 2013
- [14] A Fabry-Pérot fiber-optic ultrasonic hydrophone for the simultaneous measurement of temperature and acoustic pressure” in J. Acoust. Soc. Am, Vol. 125, No. 6, page 3611, June 2009